·Original Article·

Deglycosylation altered the gating properties of rNav1.3: glycosylation/deglycosylation homeostasis probably complicates the functional regulation of voltage-gated sodium channel

Qing XU[1*], Hui-Wen CHENG[1*], Hui-Qiong HE[2], Zhi-Rui LIU[1], Ming HE [1], Hong-Tian YANG[1], Zhi-Lei ZHOU[1], Yong-Hua JI[1]

[1]*School of Life Science, Shanghai University, Shanghai 200444, China*
[2]*Shanghai Institute of Biological Science, Chinese Academy of Science, Shanghai 200031, China*

Abstract: Objective To examine the effect of deglycosylation on gating properties of rNav1.3. **Methods** rNav1.3 was expressed in *Xenopus* oocyte, with glycosylation inhibition by using tunicamycin. Two-electrode voltage clamp was employed to record the whole-cell sodium current and data were analyzed by Origin software. Those of glycosylated rNav1.3 were kept as control. **Results** Compared with glycosylated ones, the steady-state activation curve of deglycosylated rNav1.3 was positively shifted by about 10 mV, while inactivation curve was negatively shifted by about 8 mV. **Conclusion** Glycosylation altered the gating properties of rNav1.3 and contributed to the functional diversity.

Keywords: rNav1.3; voltage-gated sodium channel; glycosylation; two-electrode voltage clamp; *Xenopus* oocyte

1 Introduction

It is well known that ion channels on the plasma membrane play a critical role in neural signal transduction. In actual fact, ion channels are subjected to posttranslational modification such as glycosylation and thus regulating the multiple functions[1]. But much less is known about oligosaccharide component than the channel protein since the first voltage-gated sodium channel was cloned[2]. The main difficulty may be the complexity of the structure of oligosaccharide[3] and lack of specific N-linked glycosylation inhibitors[4].

Glycosylation has been demonstrated to be crucial to the function of ion channels. Inhibition of N-linked glycosylation altered the voltage dependence of channel gating of Kv1.1 and KvLQT/minK (I_{sK}), and the open probability of the renal outer medullary K^+ channel ROMK1 (inward rectifier K^+ channel), as well as the pH sensitivity of KvLQT/minK channels[5,6]. N-linked glycosylation increases the stability of Shaker potassium channels but is not the acquisition of the native structure which is responsible for faster trafficking of the Shaker protein from the endoplasmatic reticulum to the Golgi[7,8], and is required for expression and stability of HERG channels in the cell membrane[9,10]. Mutations of glycosylation sites of HERG channels could cause long QT (LQT) syndrome, a HERG associated cardiac disorder[11].

Voltage-gated sodium channel (VGSC) is critical in the initiation and propagation of action potential. Compared with K^+ channels, however, the knowledge of N-linked glycosylation of Na^+ channels seems poorer. As rNav1.3 is an isoform of physiological significance, in the present study, the effect of deglycosylation of rNav1.3 was investigated.

2 Materials and methods

2.1 Plasmid The recombinant plasmid containing rNav1.3 α-subunit was kindly provided by Professor Allan Goldin, University of California, USA.

2.2 *In vitro* transcription and expression in *Xenopus* ooytes Plasmid cDNA was linearized with *N*otI and then transcribed

*The authors contributed equally to this work.
Corresponding author: Yong-Hua JI
Tel and Fax: 86-21-66135189
E-mail: yhji@staff.shu.edu.cn
Article ID:1673-7067(2008)-05-0283-05
CLC number: Q424
Document code: A
Received date: 2008-05-24

into cRNA *in vitro* using a T7 RNA polymerase Message Machine transcription kit (Ambion, Inc., Austin, TX, USA). The yield of cRNA was estimated by glyoxal gel analysis. Isolation of *Xenopus* oocytes was performed as described previously[12] with a slight modification. Briefly, *Xenopus* laevis was anesthetized by ice for about 30 min. The oocytes were removed from the ovary and washed with ORi solution (90 mmol/L NaCl, 2 mmol/L KCl, 2 mmol/L $CaCl_2$ and 5 mmol/L MOPS, pH 7.4), then incubated at 20 °C with gentle shaking for about 3 h in liberase (7 mg/mL; Sigma) solved in ORi solution. Oocytes were transferred to another clean dish filled with fresh ORi solution to remove liberase, followed by selection of healthy Stage V or VI defolliculated oocytes and injection with about 10 ng cRNA solution per ooctye. Control oocytes were injected with a corresponding volume of purified water (MilliQ, Millipore). Oocytes were cultured in a daily changed C-ORi solution (ORi plus 0.07 g/L ciprofloxacin hydrochloride) at 20 °C for 40-48 h.

2.3 Inhibition of N-linked glycosylation by tunicamycin To express deglycosylated channels in oocytes, tunicamycin, a potent inhibitor of N-linked glycosylation was employed as described by Everts *et al*.[13,14]. Briefly, at 24 h before injection with cRNA, oocytes were preinjected with 30 μg/mL tunicamycin (36.8 nL/oocyte). Immediately before injection, a stock solution of 10 mg/mL tunicamycin was produced and revolved in DMSO, which was diluted to 0.30% with purified water. DMSO of less or equal to 0.30% in concentration does little harm to oocytes. Bath treatment of oocytes with tunicamycin turned out to be largely ineffective in inhibiting N-glycosylation.

2.4 Electrophysiological recording and data analysis Two-electrode voltage clamp (TEVC) was employed to record the whole-cell sodium currents and membrane potential with TURBO TEC-03X amplifier and Cellwork 5.5 software (npi Instrument, Germany). The glass electrodes were filled with 3 mol/L KCl, linked with Ag/AgCl electrode to the detectors and balanced in ORi solution for at least 30 min before recording. The data were colleted after analog filtering at 1.3 kHz and analyzed by Origin 7.5 software. All the experiments above were performed at room temperature. The voltage dependence of activation was analyzed using a step protocol in which oocytes were depolarized from a holding potential of –100 mV to potentials ranging from –100 mV to +50 mV in 10 mV increments. Peak currents were normalized to the maximal peak current and plotted against voltage. To calculate a reversal potential, the resulting *I-V* curve of each data set was individually fit with the following equation:

$$I = \{1 + \exp[-0.04 \times z \times (V - V_{1/2})]\} - 1 \times g \times (V - V_{rev}), \quad (1)$$

where I is the current amplitude, z is the apparent gating charge, V is the potential of the given pulse, $V_{1/2}$ is the half-maximal voltage, g is a factor related to the number of open channels during the given pulse, and V_{rev} is the reversal potential. Conductance was then calculated directly using the equation:

$$G = I/(V - V_{rev}), \quad (2)$$

where G is conductance and I, V and V_{rev} are as described above. The conductance values were fit with the two-state Boltzmann equation:

$$G = 1/\{1 + \exp[-0.04 \times z \times (V - V_{1/2})]\}, \quad (3)$$

where z is the apparent gating charge, V is the potential of the given pulse, $V_{1/2}$ is the potential for half-maximal activation. The voltage dependence of steady-state inactivation was determined using a two-step protocol in which a conditioning pulse was applied from a holding potential of –100 mV to potentials ranging from –100 mV to +70 mV in 5 mV increments for 100 ms, immediately followed by test pulse to 0 mV.

The peak current amplitudes during the subsequent test pulses were normalized to the peak current amplitude during the first test pulse, plotted against the potential of the conditioning pulse, and fit with the two-state Boltzmann equation:

$$I = 1/\{1 + \exp[(V - V_{1/2})/k]\}, \quad (4)$$

where I is equal to the test pulse current amplitude, V is the potential of the conditioning pulse, $V_{1/2}$ is the voltage for half-maximal inactivation, and k is the slope factor.

Tetrodotoxin (TTX) subtraction was used to eliminate all non-TTX-sensitive currents by subtracting those currents recorded in the presence of 500 nmol/L TTX from those recorded in the absence of TTX.

Data are presented as mean±SEM. The number of examined cells was represented by n. Paired student's t-test was used for comparisons, and statistical significance was assessed as $P < 0.05$.

3 Results

3.1 Characterization of rNav1.3 sodium current After 40-48 h incubation of the cRNA of recombinant plasmid containing rNav1.3 α-subunit, the whole-cell sodium current

could be recorded (Fig. 1). The amplitude of sodium channel was about 5 000 nA and could be completely blocked by 500 nmol/L TTX, demonstrating that the current was contributed by heterologously expressed rNav1.3 in the oocyte and further experiment could be performed.

3.2 Current amplitude of glycosylated/deglycosylated rNav1.3 There was no significant difference of current amplitude between glycosylated and deglycosylated rNav1.3 as shown in Fig. 2.

3.3 The steady-state activation curve of deglycosylated rNav1.3 Compared with the glycosylated ones, the steady-state activation curve of deglycosylated rNav1.3 was positively shifted by about 10 mV and voltage constant enlarged by about 1 unit as shown in Fig. 3 and Table 1.

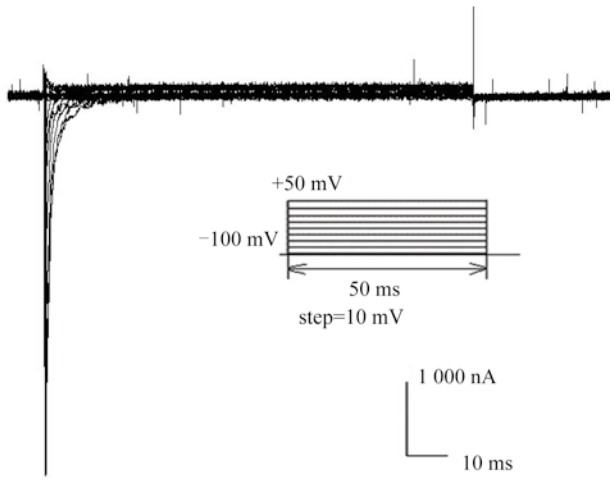

Fig. 1 Characterization of the whole-cell rNav1.3 current. After 40-48 h of incubation, the whole-cell current of rNav1.3 expressed in *Xenopus* oocytes could be evoked by a step protocol in which oocytes were depolarized from a holding potential of –100 mV to potentials ranging from –100 mV to +50 mV in 5 mV increments. The amplitude of sodium channel was about 5 000 nA.

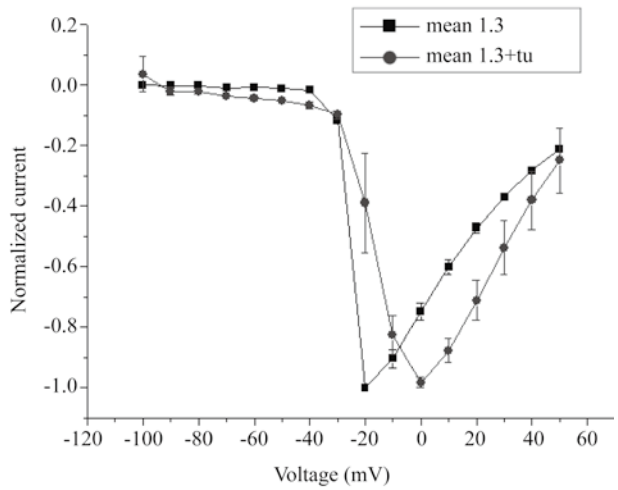

Fig. 2 Normalized *I-V* curve. The current amplitude of degclycosylated rNav1.3 (●) had no significant difference compared with that of glycosylated ones (■). (n = 9)

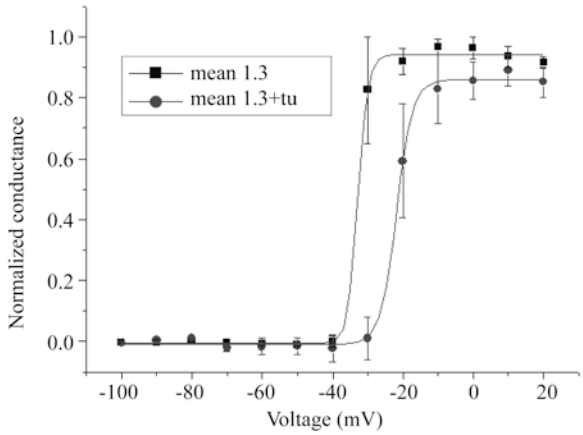

Fig. 3 The steady-state activation curve of deglycosylated rNav1.3 was positively shifted. $V_{1/2}$ value of glycosylated rNav1.3 was –32.80±1.30 (■); after deglycosylation, $V_{1/2}$ increased to 21.86±0.38 (●), $P < 0.05$. (n = 9)

Table. 1 Comparison of voltage dependence of steady-state activation between glycosylated and deglycosylated rNav1.3 (n = 9)

Channel situation	K*	$V_{1/2}$# (mV)
Glcycosylated rNav1.3	1.41±0.65	–32.80±1.30
Deglycosylated rNav1.3	2.30±0.40	–21.86±0.38

*K is the voltage constant; #$V_{1/2}$ is the voltage for half-maximal activation.

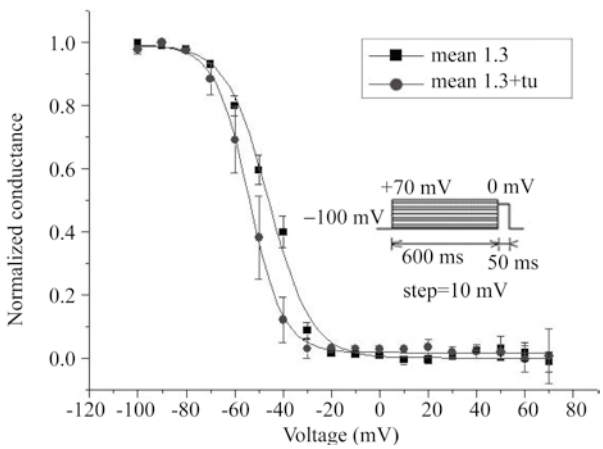

Fig. 4 The steady-state inactivation curve of deglycosylated rNav1.3 was negatively shifted. A two-step protocol was use to determined the voltage dependence of steady-state inactivation, in which a conditioning pulse was applied from a holding potential of –100 mV to potentials ranging from –100 mV to +70 mV in 5 mV increments for 100 ms, immediately followed by test pulse to 0 mV. $V_{1/2}$ value of glycosylated rNav1.3 was –45.97±0.64 (■); after deglycosylation, $V_{1/2}$ decreased to 54.13±0.57 (●), $P < 0.05$. (n = 9)

3.4 The steady-state inactivation curve of deglycosylated rNav1.3 Compared with the glycosylated ones, the steady-state inactivation curve of deglycosylated rNav1.3 was negatively shifted by about 8 mV (Fig. 4, Table 2)

Table. 2 Comparison of voltage dependence of steady-state inactivation between glycosylated and deglycosylated rNav1.3 (n = 9)

Channel situation	K*	$V_{1/2}$# (mV)
Glycosylated rNav1.3	8.78±0.56	–45.97±0.64
Deglycosylated rNav1.3	7.07±0.49	–54.13±0.57

*K is the voltage constant; #$V_{1/2}$ is the voltage for half-maximal inactivation

4 Discussion

It has been demonstrated that glycosylation is required for maintenance of functional sodium channels in neuroblastoma cells[15]. In present study, the results clearly indicated that glycosylation might be responsible for gating properties of Na^+ channels. Likewise, similar results were found in rNav1.5 and rNav1.4[16,17]. The sialic acid localized at the first domain of the channel was recognized as the prominent component of ion channel glycosylation affecting gating of voltage-dependent Na^+ channel in an isoform-specific manner[18].

It was found that the *G-V* curve of activation of rNav1.5 and rNav1.4 changed more sharply than that of inactivation by deglycosylation, but altered steady-state inactivation only for rNav1.9[19]. The present study found that deglycosylation of rNav1.3 altered both activation and inactivation to a similar extent. These results suggested that glycosylation resulted in the diverse gating properties of voltage-gated sodium channels.

It thus makes sense to scrutinize each sodium channels isoform: the effects of deglycosylation, the structure-function relationship, and the physiological significance of oligosaccharides. The particularly diverse roles of channel glycosylation may also be contributed by the unique phenomenon of glycoproteins described as micro-heterogeneity.

Finally, it may allow us to draw a conclusion that the glycosylation/deglycosylation homeostasis of Na^+ channels complicates the regulation of channel functions.

Acknowledgement: This work was supported by the National Basic Research Development Program of China (No. 2006CB500801).

References:

[1] Catterall WA. From ionic currents to molecular mechanisms: the structure and function of voltage-gated sodium channels. Neuron 2000, 26: 13-25.

[2] Noda M, Shimizu S, Tanabe T, Takai T, Kayano T, Ikeda T, *et al*. Primary structure of Electrophorus electricus sodium channel deduced from cDNA sequence. Nature 1984, 312: 121-127.

[3] Brisson JR, Carver JP. The relation of three-dimensional structure to biosynthesis in the N-linked oligosaccharides. Can J Biochem Cell Biol 1983, 61: 1067-1078.

[4] McDowell W, Schwarz RT. Dissecting glycoprotein biosynthesis by the use of specific inhibitors. Biochimie 1988, 70: 1535-1549.

[5] Schwalbe RA, Wang Z, Wible BA, Brown AM. Potassium channel structure and function as reported by a single glycosylation sequon. J Biol Chem 1995, 270: 15336-15340.

[6] Freeman LC, Lippold JJ, Mitchell KE. Glycosylation influences gating and pH sensitivity of I_{sK}. J Membr Biol 2000, 177: 65-79.

[7] Khanna R, Myers MP, Laine M, Papazian DM. Glycosylation increases potassium channel stability and surface expression in mammalian cells. J Biol Chem 2001, 276: 34028-34034.

[8] de Souza NF, Simon SM. Glycosylation affects the rate of traffic of the Shaker potassium channel through the secretory pathway. Biochemistry 2002, 41: 11351-11361.

[9] Petrecca K, Atanasiu R, Akhavan A, Shrier A. N-linked glycosylation sites determine HERG channel surface membrane expression. J Physiol 1999, 515 (Pt 1): 41-48.

[10] Gong Q, Anderson CL, January CT, Zhou Z. Role of glycosylation in cell surface expression and stability of HERG potassium channels. Am J physiol Heart Circ Physiol 2002, 283: H77-H84.

[11] Satler CA, Vesely MR, Duggal P, Ginsburg GS, Beggs AH. Multiple different missense mutations in the pore region of HERG in patients with long QT syndrome. Hum Genet 1998, 102: 265-272.

[12] Patton DE, Goldin AL. A voltage-dependent gating transition induces use-dependent block by tetrodotoxin of rat IIA sodium channels expressed in *Xenopus* oocytes. Neuron 1991, 7: 637-647.

[13] Takatsuki A, Arima K, Tamura G. Tunicamycin, a new antibiotic. I. Isolation and characterization of tunicamycin. J Antibiot (Tokyo), 24: 215-223.

[14] Everts I, Villmann C, Hollmann M. N-Glycosylation is not a prerequisite for glutamate receptor function but is essential for lectin modulation. Mol Pharmacol 1997, 52: 861-873.

[15] Waechter CJ, Schmidt JW, Catterall WA. Glycosylation is required for maintenance of functional sodium channels in neuroblastoma cells. J Biol Chem 1983, 258: 5117-5123.

[16] Ufret-Vincenty CA, Baro DJ, Lederer WJ, Rockman HA, Quinones LE, Santana LF. Role of sodium channel deglycosylation in

the genesis of cardiac arrhythmias in heart failure. J Biol Chem 2001, 276: 28197-28203.

[17] Bennett E, Urcan MS, Tinkle SS, Koszowski AG, Levinson SR. Contribution of slialic acid to the voltage dependence of sodium channel gating: a possible electrostatic mechanism. J Gen Physiol 1997, 109: 327-343.

[18] Bennett ES. Isoform-specific effects of sialic acid on voltage-dependent Na^+ channel gating: functional sialic acids are localized to the S5-S6 loop of domain I. J Physiol 2002, 538 (Pt 3): 675-690.

[19] Tyrrell L, Renganathan M, Dib-Hajj SD, Waxman SG. Glycosylation alters steady-state inactivation of sodium channel Nav1.9/NaN in dorsal root ganglion neurons and is developmentally regulated. J Neurosci 2001, 21: 9629-9637.

去糖基化改变 rNav1.3 门控性质：糖基化 / 去糖基化的动态平衡可能使电压门控钠通道的调控功能更具复杂性

徐清[1]，程慧雯[1]，何慧琼[2]，刘志睿[1]，贺明[1]，杨宏天[1]，周智磊[1]，吉永华[1]

[1]上海大学生命科学学院，上海 200444

[2]中国科学院上海生命科学研究院，上海 200031

摘要：目的 观察糖基化对 rNav1.3 电压门控性质的影响。**方法** 将 rNav1.3 在爪蟾卵母细胞中表达，衣霉素抑制其糖基化，双电极电压钳记录全细胞电流，Origin 软件分析处理数据。对照组为未去糖基化的 rNav1.3。**结果** 与糖基化的 rNav1.3 相比，去糖基化的 rNav1.3 稳态激活曲线向去极化方向偏移约 10 mV，稳态失活曲线向超极化方向偏移约 8 mV。**结论** 糖基化修饰改变 rNav1.3 的电压门控性质，异化其生理功能。

关键词：rNav1.3；电压门控钠通道；糖基化；双电极电压钳；爪蟾卵母细胞